Impact of nuclear effects on the determination of the nucleon axial mass

Omar Benhar[1] and Davide Meloni[2]
[1]*INFN and Department of Physics*
"Sapienza" Università di Roma, I-00185 Roma, Italy
[2]*Department of Physics and INFN*
Università "Roma Tre", I-00146 Roma, Italy
(Dated: March 13, 2009)

We analize the influence of nuclear effects on the determination of the nucleon axial mass from nuclear cross sections. Our work is based on a formalism widely applied to describe electron-nucleus scattering data in the impulse approximation regime. The results of numerical calculations show that correlation effects, not taken into account by the relativistic Fermi gas model, sizably affect the Q^2-dependence of the cross section. However, their inclusion does not appear to explain the large values of the axial mass recently reported by the K2K and MiniBooNE collaborations.

PACS numbers: 25.30.Pt, 13.15.+g, 24.10.Cn

Experimental searches of neutrino oscillations exploit neutrino-nucleus interactions to detect the beam particles, whose properties are largely unknown. The use of nuclear targets as detectors, while allowing for a substantial increase of the event rate, entails non trivial problems, since data analysis requires a quantitative understanding of neutrino-nucleus interactions. In view of the present experimental accuracy, the treatment of nuclear effect is in fact regarded as one of the main sources of systematic uncertainty (see, e.g., Ref.[1]).

The description of nuclear dynamics is particularly critical to analyses aimed at obtaining *nucleon* properties from *nuclear* cross sections.

Recently, the K2K [2] and MiniBooNE [3] collaborations have determined the nucleon axial mass M_A, i.e. the mass scale driving the Q^2-dependence of the dipole parametrization of the nucleon axial form factor, from neutrino interactions with oxygen and carbon, respectively. The reported value, $M_A \sim 1.2$ GeV, turn out to be significantly larger than the one previously determined from deuterium cross sections, $M_A \sim 1.0$ GeV [4]. The authors of Ref.[3] argue that the large M_A extracted from the data should be regarded as an "effective axial mass", embodying nuclear effects not included in the Relativistic Fermi Gas (RFG) model employed in their analysis. They also suggest that replacing the RFG with one of the more advanced nuclear models available in the literature [5, 6, 7, 8] may result in a value of M_A closer to that measured using deuterium.

This letter is aimed at assessing the impact of the treatment of nuclear effects on the determination of the nucleon axial mass. Our work is based on the approach described in Refs.[5, 9], in which nucleon-nucleon correlations not included in the RFG model are consistently taken into account.

Both K2K and MiniBooNE search for signatures of neutrino oscillations using Charged Current Quasi Elastic (CCQE) interactions

$$\nu_\mu + A \to \mu + p + (A-1) \ , \tag{1}$$

which are known to yield the dominant contribution to the cross section at neutrino energy $\lesssim 1.5$ GeV [10].

The differential cross section of process (1), in which a neutrino carrying four-momentum $k_\nu = (E_\nu, \mathbf{k}_\nu)$ scatters off a nuclear target producing a muon of four-momentum $k_\mu = (E_\mu, \mathbf{k}_\mu)$, while the target final state is undetected, can be written in Born approximation as

$$\frac{d^2\sigma}{d\Omega_\mu dE_\mu} = \frac{G_F^2\, V_{ud}^2}{16\,\pi^2}\,\frac{|\mathbf{k}_\mu|}{|\mathbf{k}_\nu|}\,L_{\alpha\beta}\,W_A^{\alpha\beta} \ , \tag{2}$$

where G_F is the Fermi constant and V_{ud} is the CKM matrix element coupling u and d quarks. The tensor $L_{\alpha\beta}$ is fully specified by the lepton kinematical variables, while the definition of $W_A^{\alpha\beta}$ involves the target initial and final states, as well as the nuclear weak current.

For neutrino energies larger than ~ 0.5 GeV, $W_A^{\alpha\beta}$ can be obtained within the impulse approximation (IA), i.e. assuming that neutrino-nucleus scattering reduces to the incoherent sum of scattering processes involving individual neutrons, whose momentum ($\mathbf{p}_n$) and removal energy (E) distribution is described by the nuclear spectral function $P(\mathbf{p}_n, E)$ [11, 12]. Neglecting final state interactions (FSI) between the struck nucleon and the spectator particles, the nuclear tensor can be written in the form [5, 9]

$$W_A^{\alpha\beta} \ = \ \int d^3p_n\, dE\, P(\mathbf{p}_n, E)\ W_n^{\alpha\beta}(\tilde{p}_n, \tilde{q}) \ , \tag{3}$$

where $q = k_\nu - k_\mu$ is the four-momentum transfer and $\tilde{p} = (\tilde{E}_n, \mathbf{p}_n)$, with $\tilde{E}_n \ = \ (m_n^2 + |\mathbf{p}_n|^2)^{1/2}$, m_n being the neutron mass.

The tensor $W_n^{\alpha\beta}$ describes the charged current weak interactions of a neutron of initial momentum $\mathbf{p}_n$ *in free space*. The effect of nuclear binding is accounted for by the replacement $q \to \tilde{q} \equiv (\tilde{q}_0, \mathbf{q})$, with

$$\begin{aligned} \tilde{q}_0 \ &= \ q_0 + M_A - E_{A-1} - \tilde{E}_n \\ &= \ \sqrt{m_p^2 + |\mathbf{p}_n + \mathbf{q}|^2} - \sqrt{m_n^2 + |\mathbf{p}_n|^2} \ , \end{aligned} \tag{4}$$

where M_A and $E_{A-1} = [(M_A - m_n + E)^2 + |\mathbf{p}_n|^2]^{1/2}$ denote the target mass and the energy of the recoiling nucleus, respectively [9].

The above procedure, originally proposed in the context of a study of electron induced nucleon knock out processes [14], accounts for the fact that a fraction of the energy transfer to the target goes into excitation energy of the spectator system. The energy $\delta q_0 = q_0 - \tilde{q}_0$ is spent to put the struck particle on the mass shell, and the elementary scattering process is described using free space kinematics with energy transfer $\tilde{q}_0$. The physical intepretation of $\tilde{q}_0$ emerges most clearly in the $(|\mathbf{p}_n|/m_n) \to 0$ limit, corresponding to $\tilde{q}_0 = q_0 - E$.

The main effect of FSI on the differential inclusive cross section is a redistribution of the strength, resulting from the coupling of the one particle-one hole final state to more complex n-particle n-hole configurations [15]. This leads to a sizable quenching of the cross section in the region of the quasi free peak, corresponding to $q_0 \sim Q^2/2m_n$, with $Q^2 = -q^2$, associated with the enhancement of the tails at both low and high q_0.

In this work FSI have been described following the approach originally developed in Ref.[15], in which the inclusive cross section is written in the convolution form

$$\frac{d\sigma}{d\Omega_\mu dE_\mu} = \int dE'_\mu \left(\frac{d\sigma_0}{d\Omega_\mu dE'_\mu}\right) f(E_\mu - E'_\mu) \ , \quad (5)$$

where $(d\sigma_0/d\Omega_\mu dE'_\mu)$ is the cross section in the absence of FSI , obtained from Eqs.(2) and (3). The folding function, embodying FSI effects, is trivially related to the spectral function of particle states [16]. It can be computed using the formalism of nuclear many-body theory and the eikonal approximation, i.e. assuming that: i) the outgoing proton moves along a straight trajectory with constant speed, and ii) the spectator nucleons act as a collection of fixed scattering centers [5, 15].

The results of Ref.[5] show that inclusion of FSI effects is needed to reproduce the measured cross sections of the process $e + ^{16}O \to e' + X$ at electron beam energy ~ 1 GeV.

In order to assess the validity of the analysis of Refs.[2, 3] and the role of nuclear effects not taken into account by the RFG model, we have first studied the dependence on M_A of the Q^2-distribution of the process $\nu_\mu + ^{16}O \to \mu + p + (A-1)$ at beam energy E_ν =1.2 GeV, corresponding to the peak in the energy spectrum of the neutrinos used by the K2K collaboration [2].

In Fig. 1 we compare the RFG results to those obtained using Eqs.(2) and (3) and the spectral function of Ref.[12], with $M_A = 1.0$ and 1.2.

It clearly appears that, while increasing the axial mass leads to an enhancement of the cross section, the inclusion of correlation effects through the use of a realistic spectral function produces a sizable quenching. The dashed line, corresponding to the model of Refs.[5, 9], turns out to be below the dot-dash line, corresponding to the RFG model, over the whole Q^2 range. Note that FSI effetcs, not taken into account in the calculations, lead to a further suppression of the curves labelled SF.

Based on the results of Fig. 1, we conclude that, as far as the Q^2 distribution at fixed neutrino energy is concerned, a larger value of the axial mass cannot be explained by replacing the RFG with the more advanced model of nuclear dynamics discussed in Refs.[5, 9].

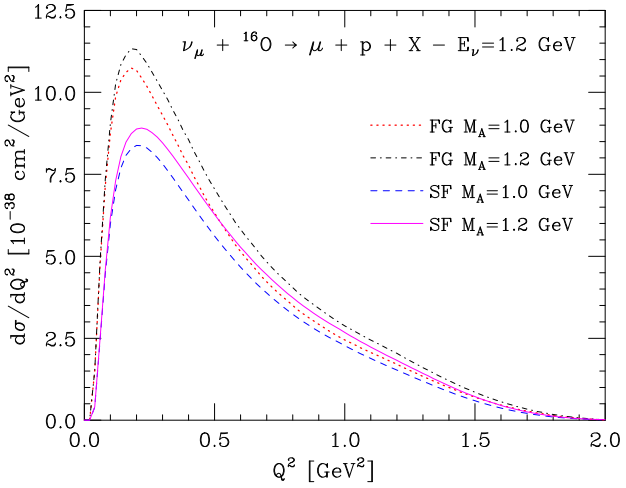

FIG. 1: (Color online) Q^2-dependence of the cross section of the process $\nu_\mu + ^{16}O \to \mu + p + X$, for neutrino energy $E_\nu = 1.2$ GeV. The dashed and solid lines, labeled SF, have been obtained using the approach of Refs.[5, 9] with M_A = 1.0 and 1.2 GeV, respectively. The corresponding results of the RFG model, with Fermi momentum $p_F = 225$ MeV and removal energy $\epsilon = 27$ MeV, are represented by the dotted and dot-dash lines, labeled FG.

It is important to realize, however, that using a realistic momentum and removal energy distribution may also significanltly affect the determination of E_ν.

From the requirement that the elementary scattering process, $\nu_\mu + n \to \mu + X$, be elastic, i.e. that

$$(k_\nu + p_n - k_\mu)^2 = m_p^2 \ , \quad (6)$$

where m_p is the proton mass and the four momentum of the struck nucleon is given by $p_n = (E_n, \mathbf{p}_n)$, with $E_n = M_A - E_{A-1}$, it follows that

$$E_\nu = \frac{m_p^2 - m_\mu^2 - E_n^2 + 2E_\mu E_n - 2\mathbf{k}_\mu \cdot \mathbf{p}_n + |\mathbf{p}_n^2|}{2(E_n - E_\mu + |\mathbf{k}_\mu| \cos\theta_\mu - |\mathbf{p}_n| \cos\theta_n)} \ , \quad (7)$$

where θ_μ is the muon angle relative to the neutrino beam and $\cos\theta_n = (\mathbf{k}_\nu \cdot \mathbf{p}_n)/(|\mathbf{k}_\nu||\mathbf{p}_n|)$.

Setting $|\mathbf{p}_n| = 0$ and fixing the neutron removal energy to a constant value ϵ, i.e. setting $E = \epsilon$, implying in turn $E_n = m_n - \epsilon$, Eq.(7) reduces to

$$E_\nu = \frac{2E_\mu(m_n - \epsilon) - (\epsilon^2 - 2m_n\epsilon + m_\mu^2 + \Delta m^2)}{2(m_n - \epsilon - E_\mu + |\mathbf{k}_\mu| \cos\theta_\mu)} \ , \quad (8)$$

with $\Delta m^2 = m_n^2 - m_p^2$. In the analysis of both K2K and MiniBooNE data, the energy of the incoming neutrino has been reconstructed using the above equation (compare to Eq.(5) of Ref.[2] and Eq.(3) of Ref.[3]), with ϵ = 27 and 34 MeV for oxygen [2] and carbon [3], respectively.

Equation(7) clearly shows that, in general, the knowledge of E_μ and θ_μ, the observables measured by K2K and MiniBooNE, *does not* uniquely determine the neutrino energy. For any given E_μ and θ_μ, E_ν depends on both magnitude and direction of the neutron momentum $\mathbf{p}_n$, as well as on its removal energy E, entering the defintion of E_n.

The distribution of neutrino energy can be obtained from Eq.(7) using values of $|\mathbf{p}_n|$ and E sampled from the probability distribution $|\mathbf{p}_n|^2 P(\mathbf{p}_n, E)$ and assuming that the polar and azimuthal angles specifying the direction of the neutron momentum be uniformly distributed.

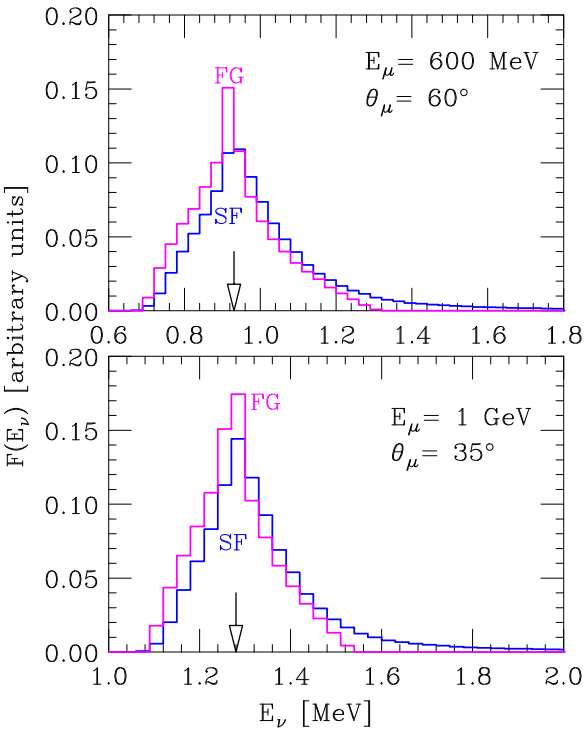

FIG. 2: (Color online) Upper panel: Neutrino energy distribution at $E_\mu = 600$ MeV and $\theta_\mu = 60°$, reconstructed from Eq.(7) using 2 $\times 10^4$ pairs of $(|\mathbf{p}_n|, E)$ values sampled from the probability distributions associated with the oxygen spectral function of Ref.[12] (SF) and the Fermi gas model, with Fermi momentum $p_F = 225$ MeV and removal energy $\epsilon = 27$ MeV(FG). The arrow points to the value of E_ν obtained from Eq. (8). Lower panel: Same as the upper panel, but for $E_\mu = 1$ GeV and $\theta_\mu = 35°$.

The spectral functions of nuclei ranging from carbon to gold, computed in Ref.[12], exhibit high momentum and high removal energy tails, extending well above $|\mathbf{p}_n| \gtrsim 500$ MeV and $E \gtrsim 100$ MeV. A direct measurement of the carbon spectral function from the $(e, e'p)$ cross section at missing momentum and energy up to ~ 800 MeV and ~ 200 MeV, respectively, has been recently carried out at Jefferson Lab [17]. The preliminary results of data analysis appear to be consistent with the theoretical predictions of Ref.[12]. On the other hand, in the RFG model the typical Fermi momentum, p_F, and average removal energy (ϵ of Eq.(8)) are ~ 200 MeV and ~ 30 MeV, respectively.

To gauge the effect of the high momentum and high removal energy tails of $P(\mathbf{p}_n, E)$, we have computed the neutrino energy distribution, $F(E_\nu)$, using 2 $\times 10^4$ pairs of $(|\mathbf{p}_n|, E)$ values drawn from the probability distributions associated with the oxygen spectral functions of both Ref.[12] and the RFG model, with Fermi momentum $p_F = 225$ MeV and removal energy $\epsilon = 27$ MeV. The results corresponding to $E_\mu = 600$ MeV and $\theta_\mu = 35°$, and $E_\mu = 1$ GeV and $\theta_\mu = 35°$, are displayed in the upper and lower panels of Fig. 2, respectively.

It appears that the distributions predicted by the RFG model are more sharply peaked at the neutrino energy given by Eq.(8). On the other hand, the $F(E_\nu)$ obtained from the spectral function of Ref.[12] are shifted towards higher energy by ~ 20 MeV, with respect to the RFG results, and exhibit a tail extending to very large values of E_ν.

The average values of E_ν calculated using the RFG distribution turn out to be $\langle E_\nu \rangle = 1.28$ GeV and 934 Mev for the kinematics of the upper and lower panels, respectively, to be compared with 1.28 GeV and 931 Mev resulting from Eq.(8). On the other hand, the distributions associated with the spectral functions of Ref.[12] yield $\langle E_\nu \rangle = 1.35$ GeV and 1.01 Gev.

As Q^2 grows with E_ν according to

$$Q^2 = 2E_\nu E_\mu \left(1 - \frac{p_\mu}{E_\mu}\cos\theta_\mu\right) - m_\mu^2 \ , \qquad (9)$$

the results of Fig. 1 and 2 suggest that using neutron energies and momenta obtained from a realistic spectral function in the equation determining the kinematics of the CCQE process would lead to extract an even larger value of the axial mass.

The energy and momentum distribution of the struck neutron also affects the weak interaction vertex, since the neutrino interacts with a *bound moving* neutron. As pointed out above, within the IA formalism binding is taken into account through a shift of the energy transfer. As a result, within the approach of Refs.[5, 9] the elementary neutrino-neutron scattering process takes place at $\tilde{Q}^2 = |\mathbf{q}|^2 - \tilde{q}_0^2 > Q^2$.

In order to assess the full impact of replacing the RFG model with the approach of Refs.[5, 9], we have computed the differential cross section of the process $\nu_\mu + A \to \mu + p + (A-1)$, as a function of the incoming neutrino energy E_ν, for the muon kinematics of Fig. 2.

The solid lines of Fig. 3 show the results of the full calculation, carried out using the spectral function of Ref.[12], while the dashed lines have been obtained neglecting the effects of FSI and the dot-dash lines correspond to the RFG model. Note that, unlike the histograms of Fig. 2, the curves displayed in Fig. 3 have different normalizations. As in Fig. 2, the arrows point to the values of E_ν given by Eq.(8).

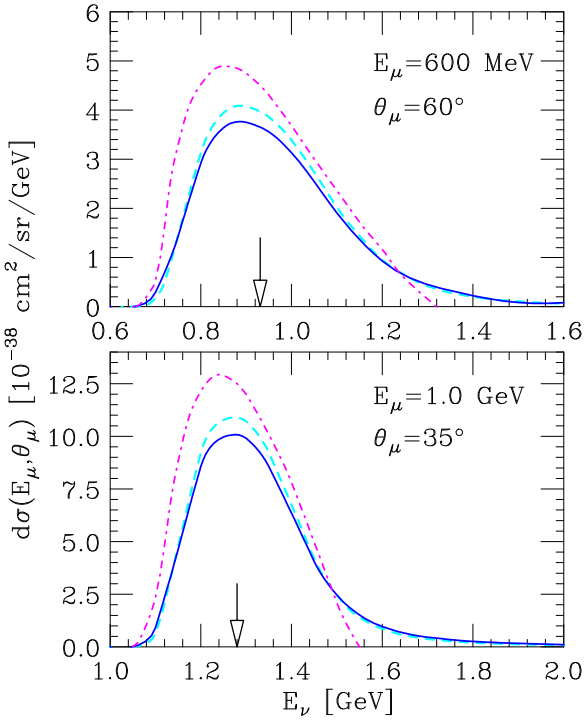

FIG. 3: (Color online) Upper panel: Differential cross section of the process $\nu_\mu + A \to \mu + p + (A-1)$, at $E_\mu = 600$ MeV and $\theta_\mu = 60^\circ$, as a function of the incoming neutrino energy. The solid line shows the results of the full calculation, carried out within the approach of Refs. [5, 9], whereas the dashed line has been obtained neglecting the effects of FSI. The dot-dash line corresponds to the RFG model with Fermi momentum $p_F = 225$ MeV and removal energy $\epsilon = 27$ MeV. The arrow points to the value of E_ν obtained from Eq. (8). Lower panel: Same as the upper panel, but for $E_\mu = 1$ GeV and $\theta_\mu = 35^\circ$.

The differences between the results of the approach of Refs. [5, 9] and those of the RFG model appear to be sizable. The overall shift towards high energies and the tails at large E_ν, present in the histograms of Fig. 2, are still clearly visible and comparable in size, while the quenching with respect to the RFG model is larger than in Fig. 2. Comparison between the dashed and dot-dash lines indicate that the ~ 20 % difference at the peak of the distributions is mainly due to the replacement $Q^2 \to \tilde{Q}^2$, while inclusion of FSI effects leads to a further reduction of about 8%.

In conclusion, the results discussed in this paper indicate that nuclear effects not included in the RFG model significantly affect the Q^2-dependence of CCQE neutrino-nucleus interactions. However, contrary to the expectation of the authors of Ref.[3], their inclusion does not help to reconcile the large values of M_A reported in Refs.[2, 3] with those extracted from deuterium data. Using the model of Refs.[5, 9] in the data analysis would in fact lead to predict an even larger value of the axial mass.

Other possible explanations of the disagreement between the values of M_A obtained by different experiments, such as misidentification of CCQE events, should be carefully investigated using state-of-the-art models of nuclear structure and dynamics.

While this paper was being drafted, the NOMAD collaboration released the results of the analysis of quasi-elastic muon neutrino and antineutrino scattering data, yielding an axial mass $M_A = 1.05 \pm 0.02(stat) \pm 0.06(syst)$ GeV [18]. As the NOMAD experiment takes data at beam energies much larger than those used in both K2K and MiniBooNE, we have chechek the sensitivity of our results to the incoming neutrino energy. It turns out thet the main features of the Q^2-distribution of the process $\nu_\mu + {}^{16}O \to \mu + p + (A-1)$ do not change significantly as E_ν increases from 1.2 GeV to 10 GeV.

The authors are indebted to M. Sakuda, for drawing their attention to the subject of this paper. Useful discussions with L. Ludovici, M.H. Shaevitz and M.O. Wascko are also gratefully acknowledged.

[1] Proceedings of NUINT07, Eds. G.P. Zeller, J.G. Morfin and F. Cavanna, AIP Conf. Proc. **967** (2007).
[2] R. Gran *et al.* (K2K Collaboration), Phys. Rev. D **74**, 052002 (2006).
[3] A.A. Aguilar Arevalo *et al.* (MiniBooNE), Phys. Rev. Lett. **98**, 231801 (2008).
[4] V. Bernard *et al.*, J. Phys. G **28**, R1 (2002).
[5] O. Benhar *et al.*, Phys. Rev. D **72**, 053005 (2005).
[6] S. Ahmad *et al.*, Phys. Rev. D **74**, 073008 (2006).
[7] J.E. Amaro *et al.*, Phys. Rev. C **71**, 015501 (2005).
[8] T. Leitner *et al.*, Phys. Rev. C **73**, 065502 (2006).
[9] O. Benhar and D. Meloni, Nucl. Phys. **A789**, 379 (2007).
[10] P. Lipari, M. Lusignoli and F. Sartogo, Phys. Rev. Lett. **74**, 4384 (1995).
[11] O. Benhar, A. Fabrocini and S. Fantoni, Nucl. Phys. **A505**, 267 (1989).
[12] O. Benhar, A. Fabrocini, S. Fantoni and I. Sick, Nucl. Phys. **A579**, 493 (1994).
[13] O. Benhar, D. Day and I. Sick, Rev. Mod. Phys. **80** (2008) 189.
[14] T. de Forest Jr., Nucl. Phys. **A392**, 232 (1983).
[15] O. Benhar *et al*, Phys. Rev. C **44**, 2328 (1991).
[16] O. Benhar, AIP Conf. Proc. **967** (2007) 111.
[17] D. Rohe *et al.* (JLab E97-006 Collaboration), Phys. Rev. Lett. **93**, 182501 (2004).
[18] NOMAD Collaboration, V. Lyubushkin *et al*, arXiv:0812.4543